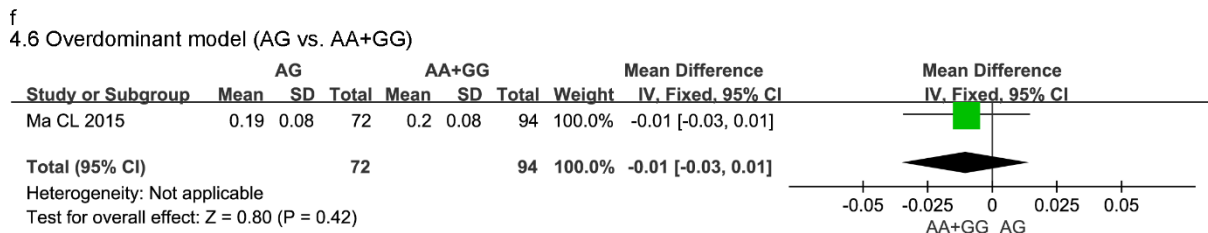
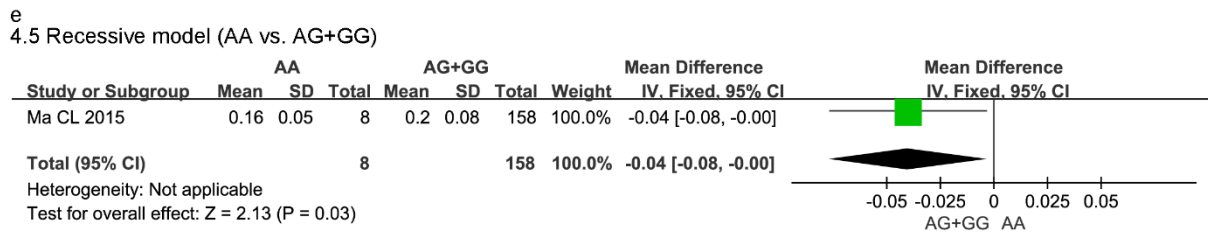
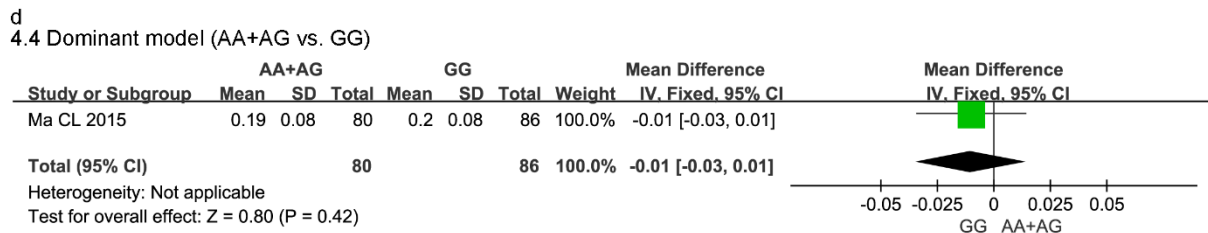
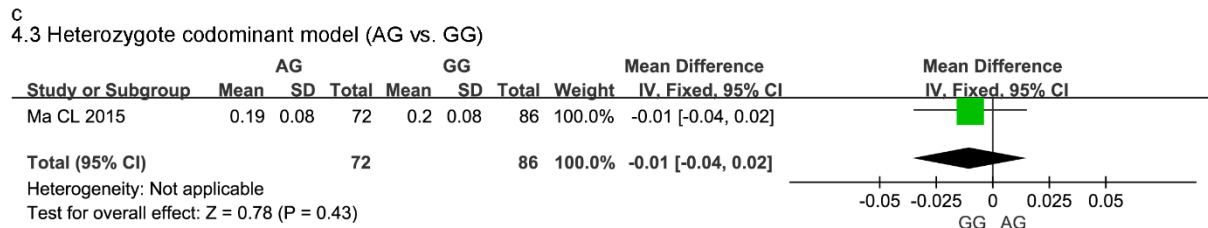
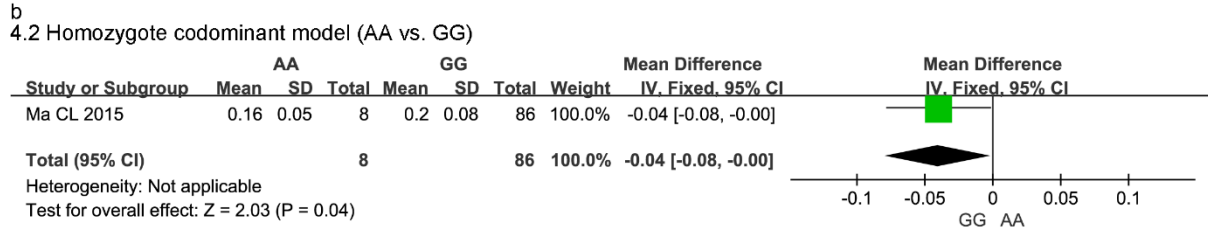
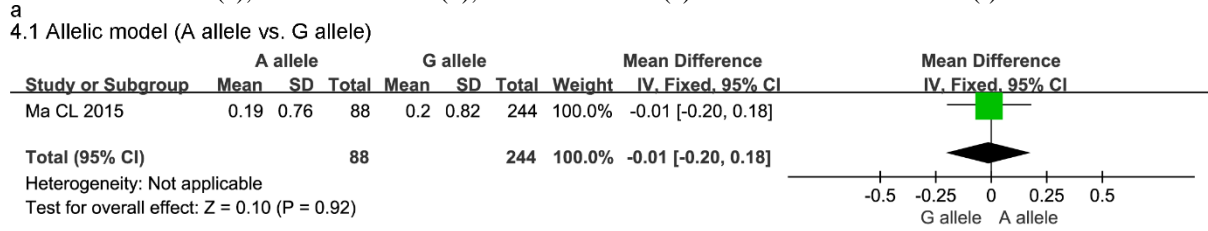


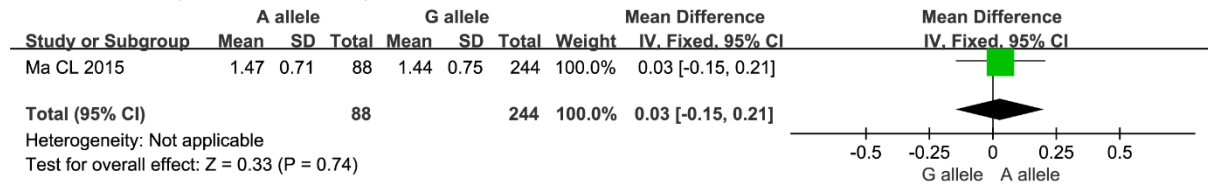
Supplemental Fig. S.1 Forest plot for association between CYP3A4 rs2242480 polymorphism and plasma concentration of CBZE to CBZ ratio in allelic model (a), homozygote codominant model (b), heterozygote codominant model (c), dominant model (d), recessive model (e) and overdominant model (f).



Supplemental Fig. S.2 Forest plot for association between CYP3A4 rs2242480 polymorphism and plasma CBZE concentration in allelic model (a), homozygote codominant model (b), heterozygote codominant model (c), dominant model (d), recessive model (e) and overdominant model (f).

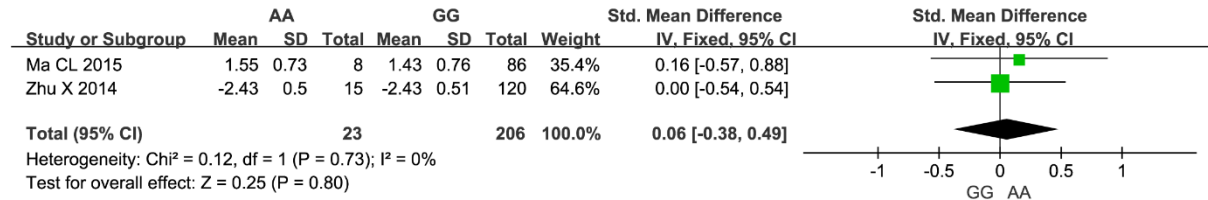
a

2.1 Allelic model (A allele vs. G allele)



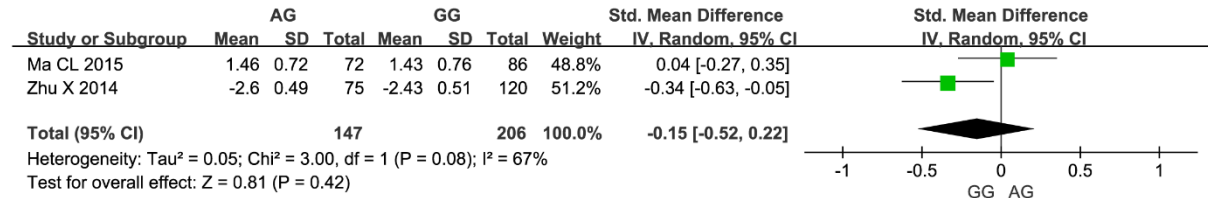
b

2.2 Homozygote codominant model (AA vs. GG)



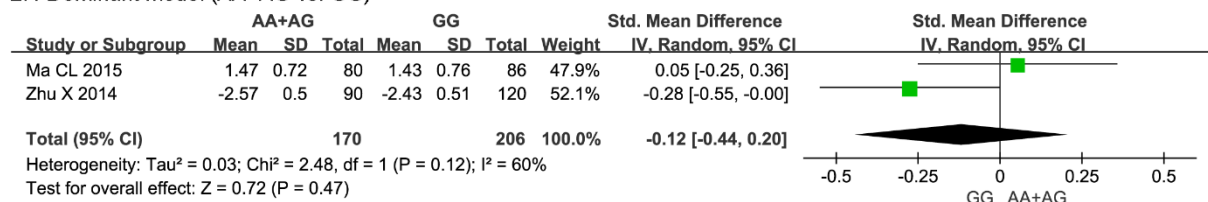
c

2.3 Heterozygote codominant model (AG vs. GG)



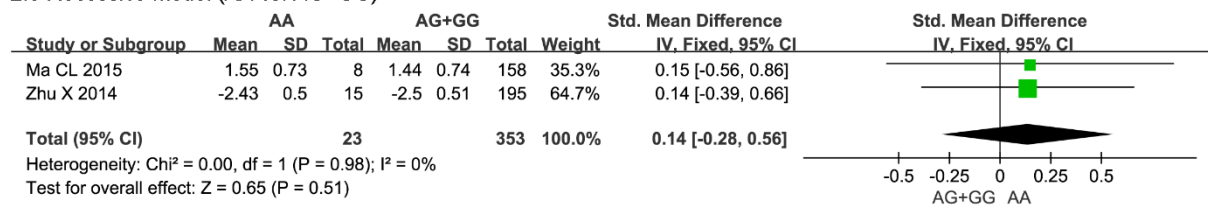
d

2.4 Dominant model (AA+AG vs. GG)



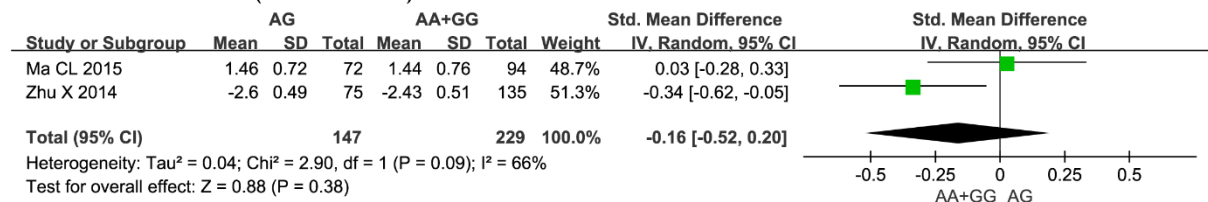
e

2.5 Recessive model (AA vs. AG+GG)

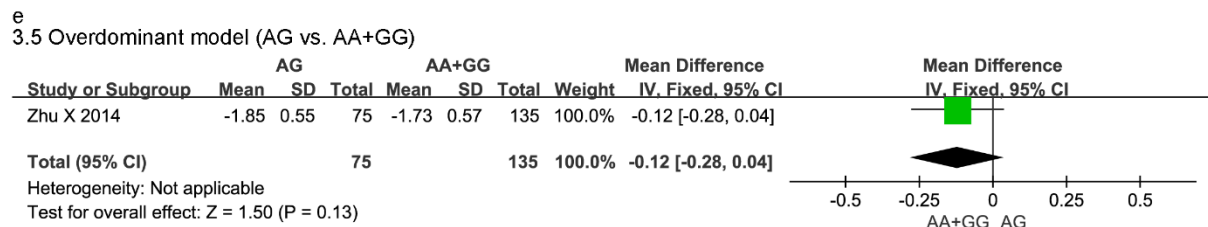
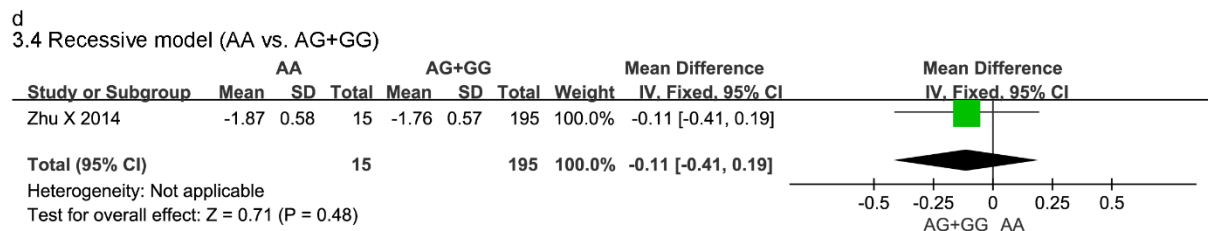
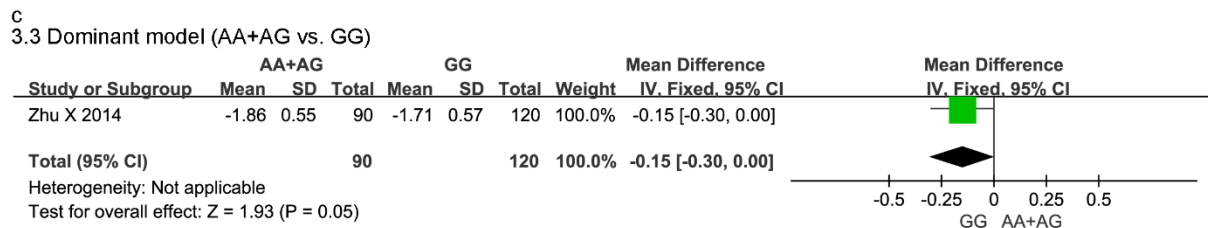
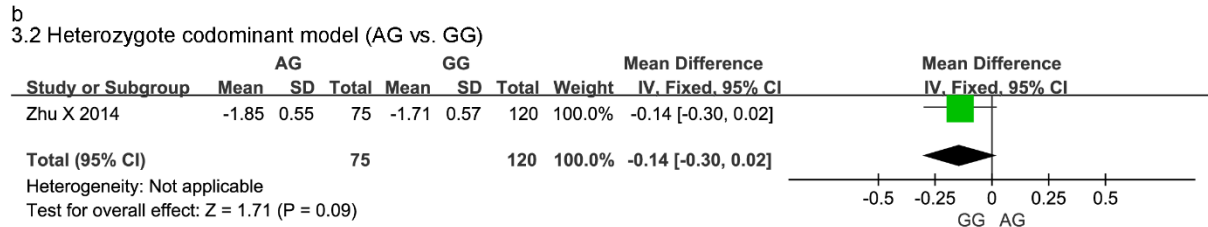
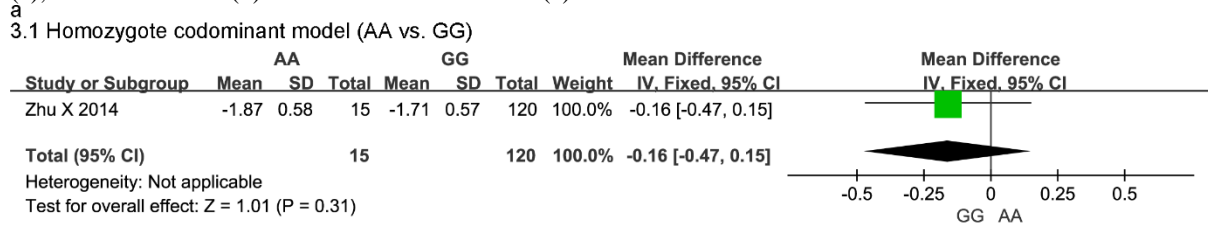


f

2.6 Overdominant model (AG vs. AA+GG)

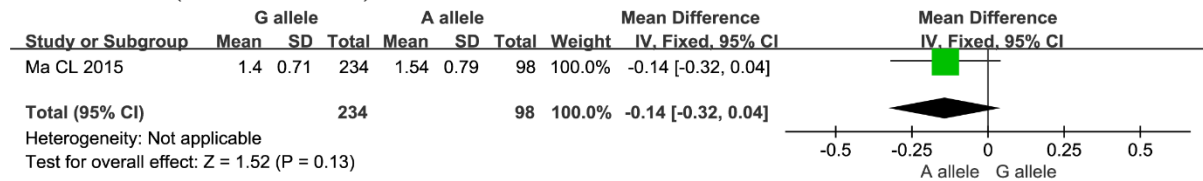


Supplemental Fig. S.3 Forest plot for association between CYP3A4 rs2242480 polymorphism and plasma CBZD concentration in homozygote codominant model (a), heterozygote codominant model (b), dominant model (c), recessive model (d) and overdominant model (e).

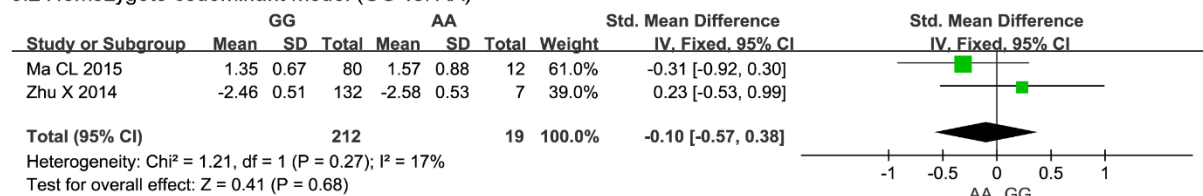


Supplemental Fig. S.4 Forest plots for association between CYP3A5 rs776746 polymorphism and plasma CBZE concentration in allelic model (a), homozygote codominant model (b), heterozygote codominant model (c), dominant model (d), recessive model (e) and overdominant model (f). Sensitivity analysis for effect of CYP3A5 rs776746 polymorphism on plasma CBZE concentration in recessive model (g).

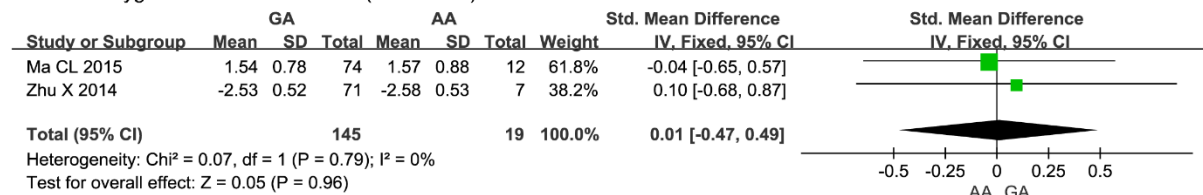
a
6.1 Allelic model (G allele vs. A allele)



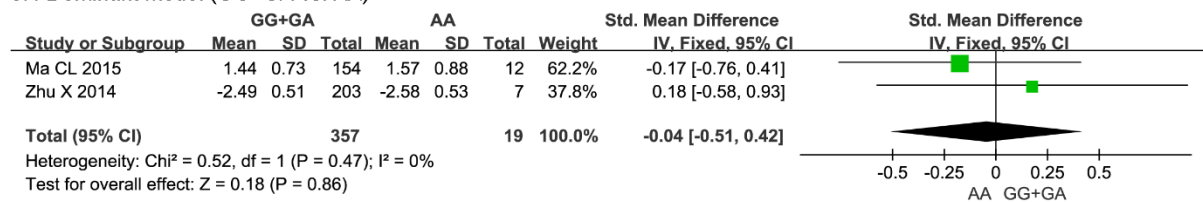
b
6.2 Homozygote codominant model (GG vs. AA)



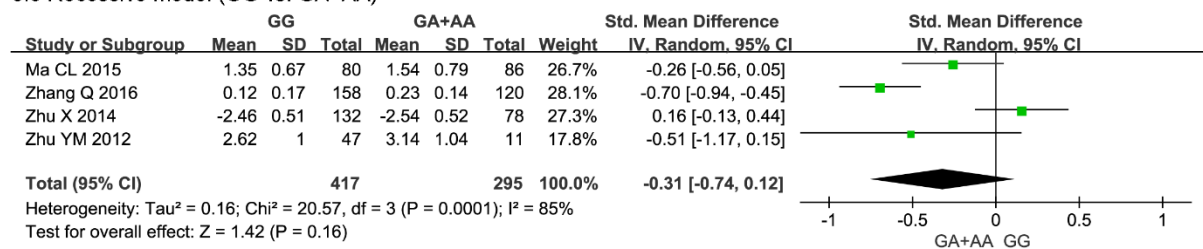
c
6.3 Heterozygote codominant model (GA vs. AA)



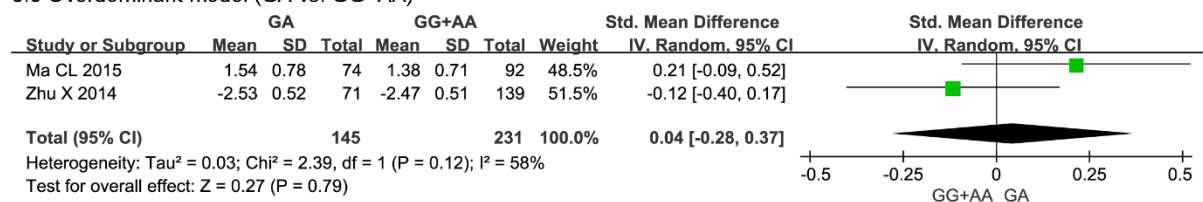
d
6.4 Dominant model (GG+GA vs. AA)



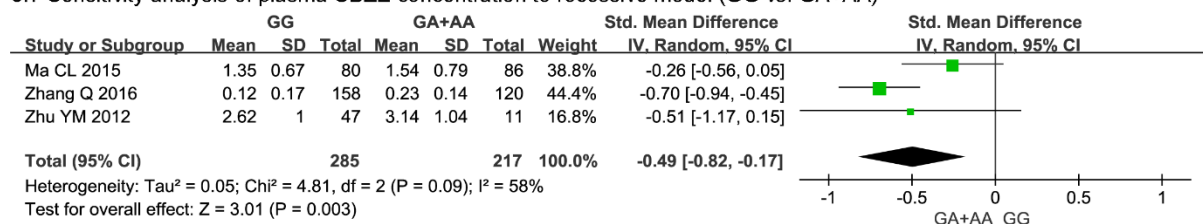
e
6.5 Recessive model (GG vs. GA+AA)



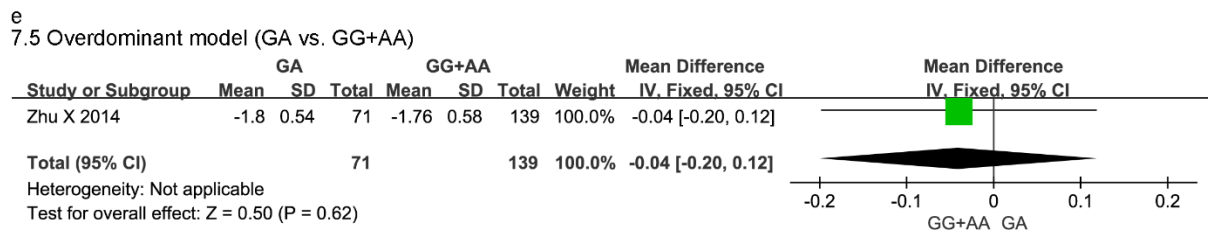
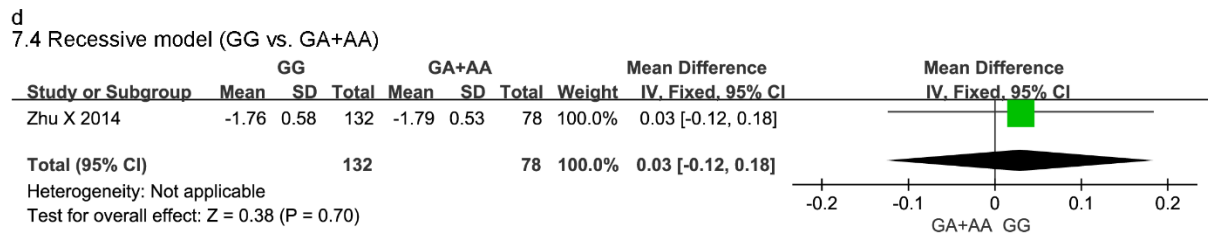
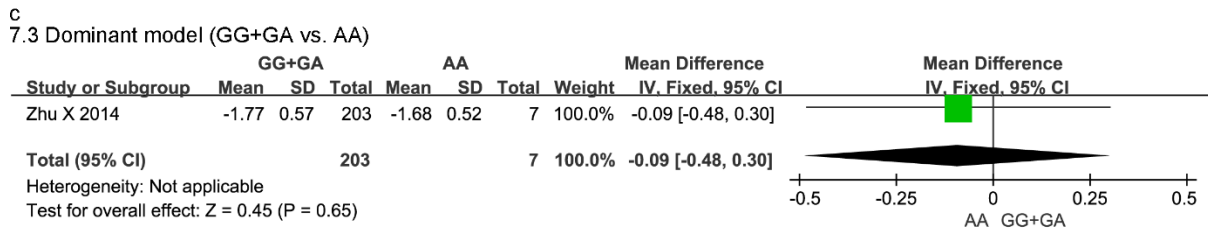
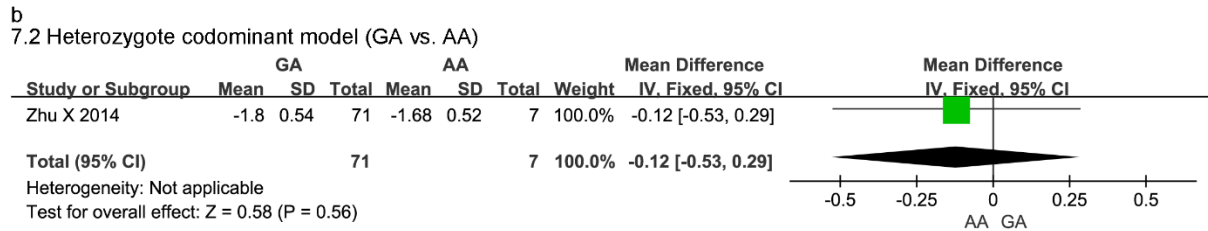
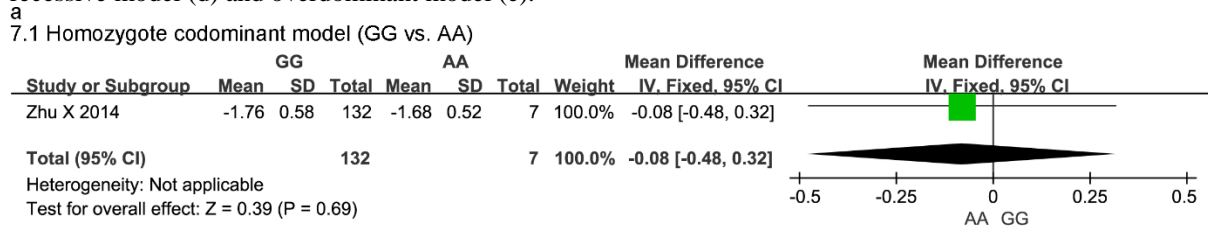
f
6.6 Overdominant model (GA vs. GG+AA)



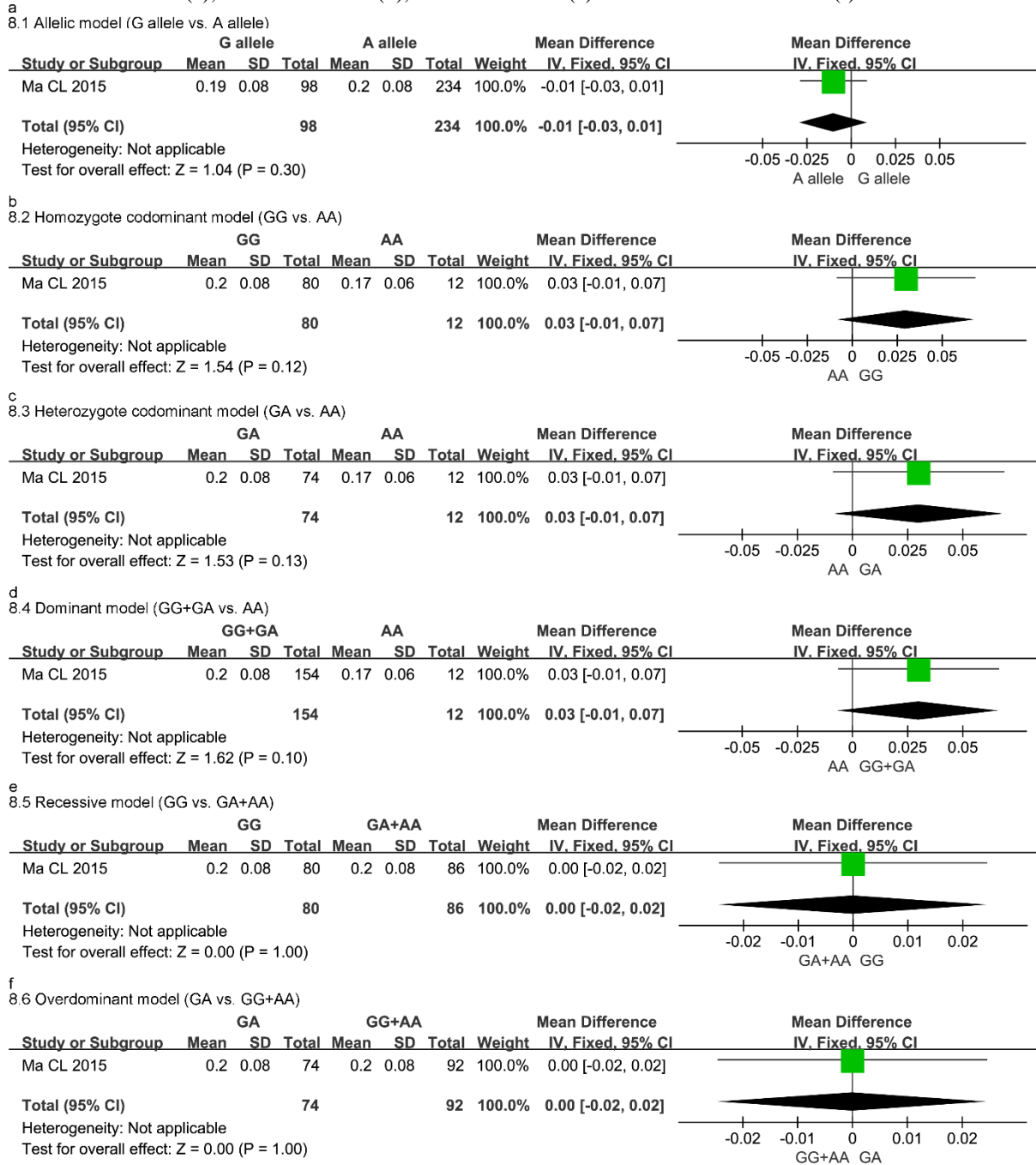
g
6.7 Sensitivity analysis of plasma CBZE concentration to recessive model (GG vs. GA+AA)



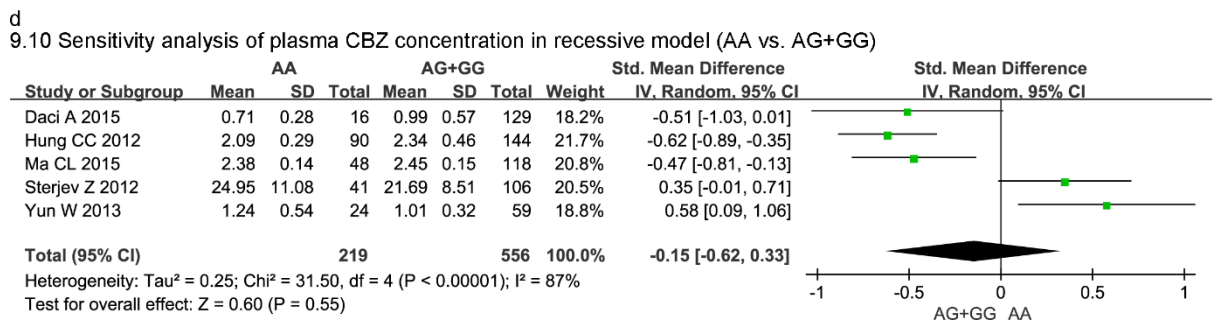
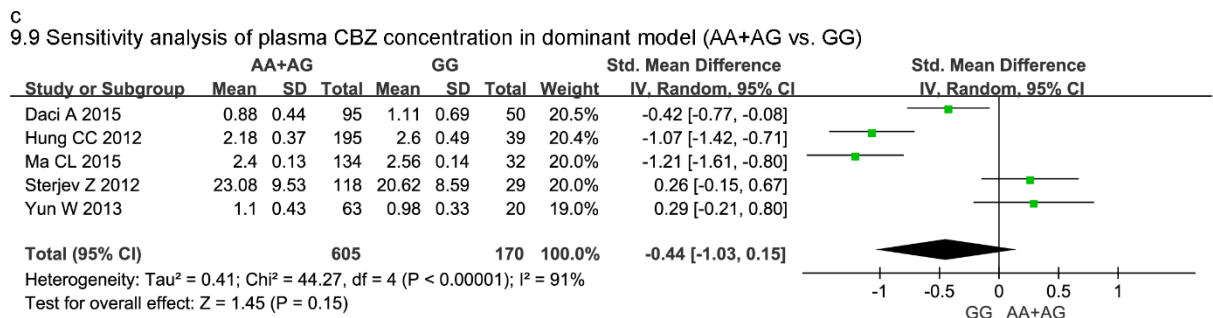
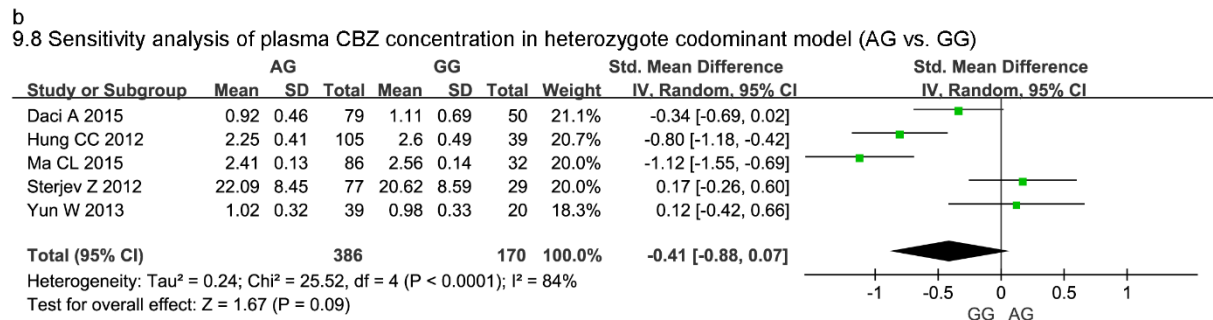
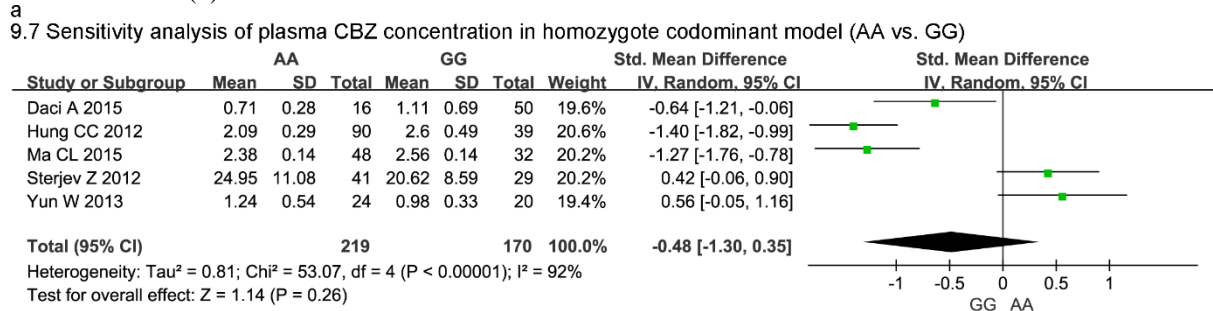
Supplemental Fig. S.5 Forest plot for association between CYP3A5 rs776746 polymorphism and plasma CBZD concentration in homozygote codominant model (a), heterozygote codominant model (b), dominant model (c), recessive model (d) and overdominant model (e).



Supplemental Fig. S.6 Forest plot for association between CYP3A5 rs776746 polymorphism and plasma concentration of CBZD to CBZ ratio in allelic model (a), homozygote codominant model (b), heterozygote codominant model (c), dominant model (d), recessive model (e) and overdominant model (f).



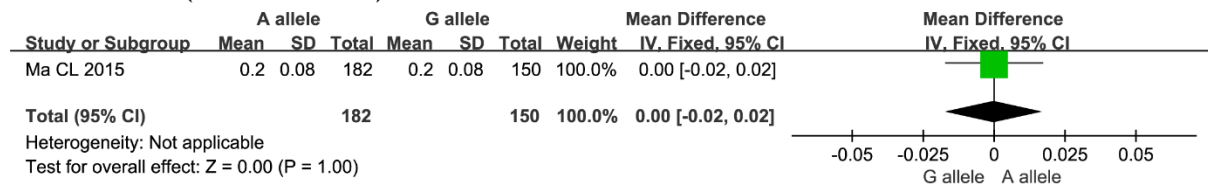
Supplemental Fig. S.7 Sensitivity analysis for effect of SCN1A rs3812718 polymorphism on plasma CBZ concentration in homozygote codominant model (a), heterozygote codominant model (b), dominant model (c) and recessive model (d).



Supplemental Fig. S.8 Forest plot for association between SCN1A rs3812718 polymorphism and plasma concentration of CBZE to CBZ ratio in allelic model (a), homozygote codominant model (b), heterozygote codominant model (c), dominant model (d), recessive model (e) and overdominant model (f).

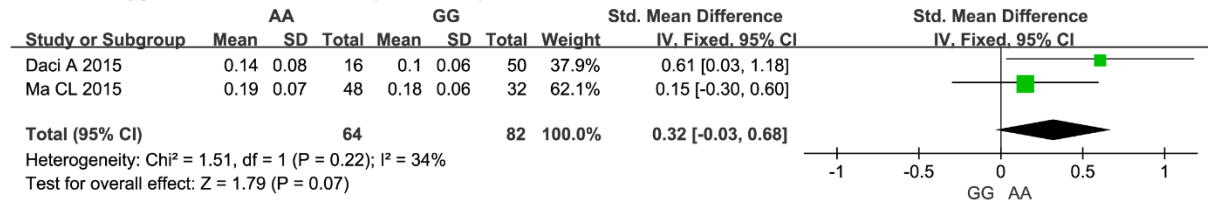
a

12.1 Allelic model (A allele vs. G allele)



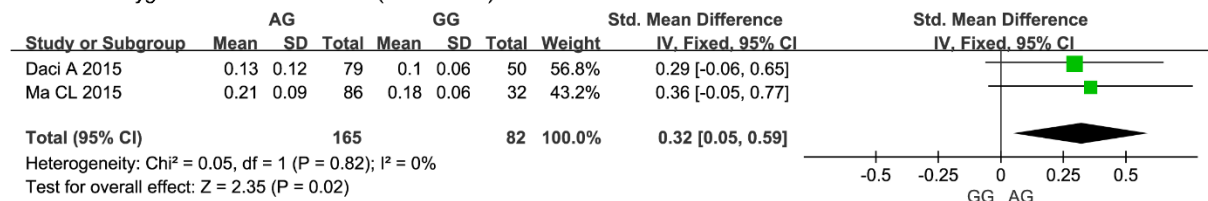
b

12.2 Homozygote codominant model (AA vs. GG)



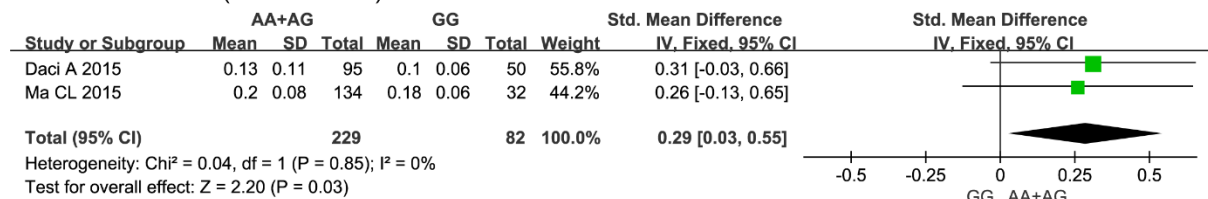
c

12.3 Heterozygote codominant model (AG vs. GG)



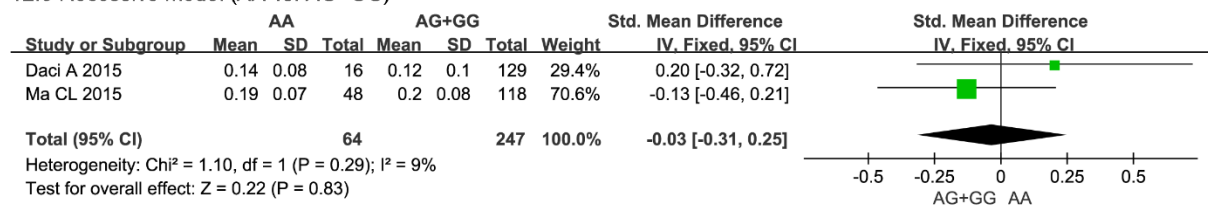
d

12.4 Dominant model (AA+AG vs. GG)



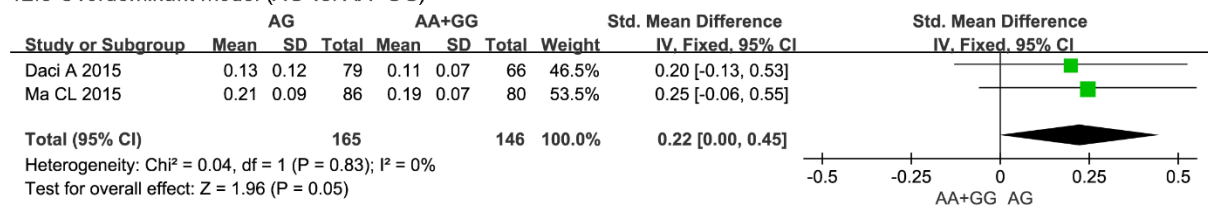
e

12.5 Recessive model (AA vs. AG+GG)



f

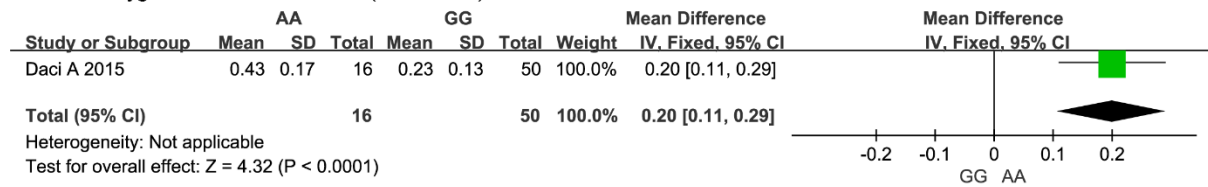
12.6 Overdominant model (AG vs. AA+GG)



Supplemental Fig. S.9 Forest plot for association between SCN1A rs3812718 polymorphism and plasma concentration of CBZD to CBZ ratio in homozygote codominant model (a), heterozygote codominant model (b), dominant model (c), recessive model (d) and overdominant model (e).

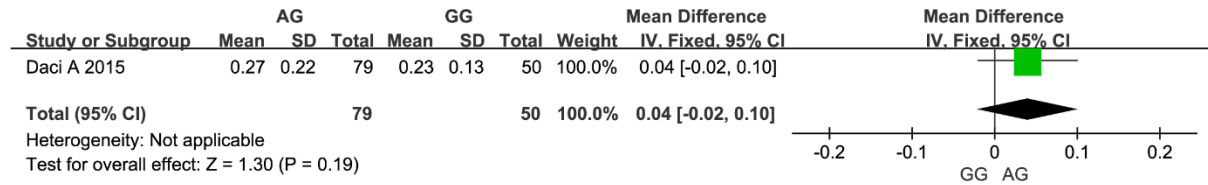
a

13.1 Homozygote codominant model (AA vs. GG)



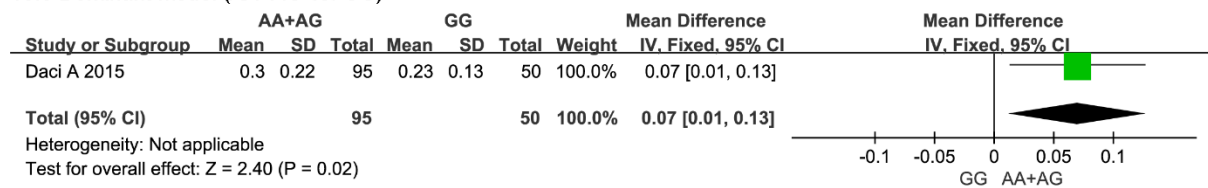
b

13.2 Heterozygote codominant model (AG vs. GG)



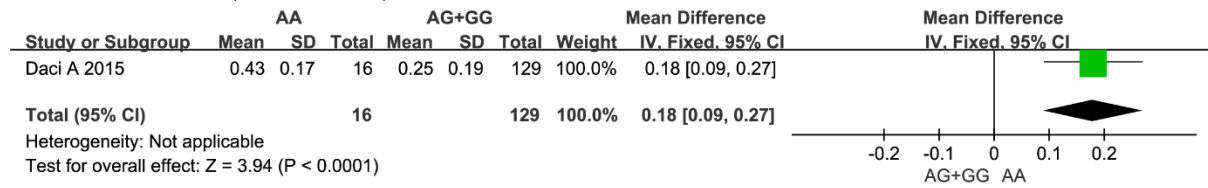
c

13.3 Dominant model (AA+AG vs. GG)



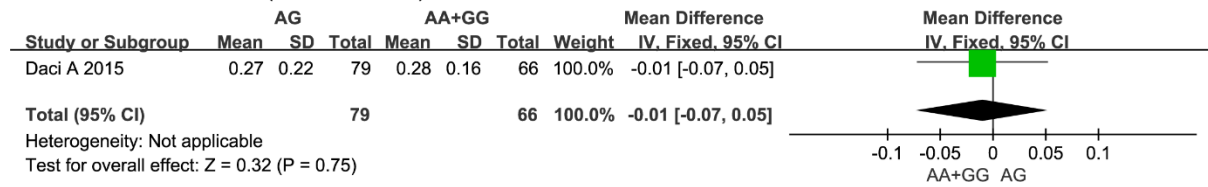
d

13.4 Recessive model (AA vs. AG+GG)

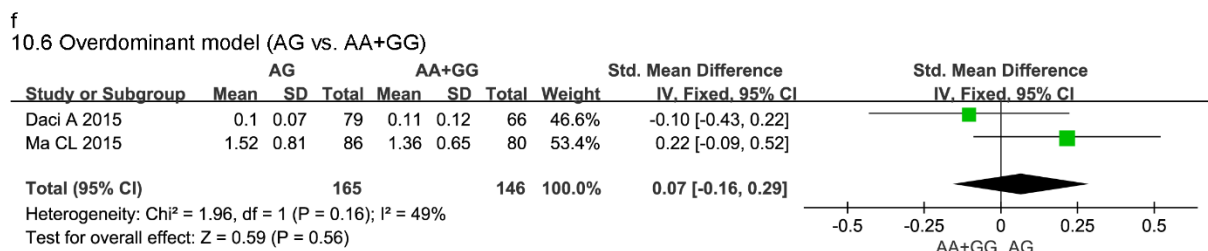
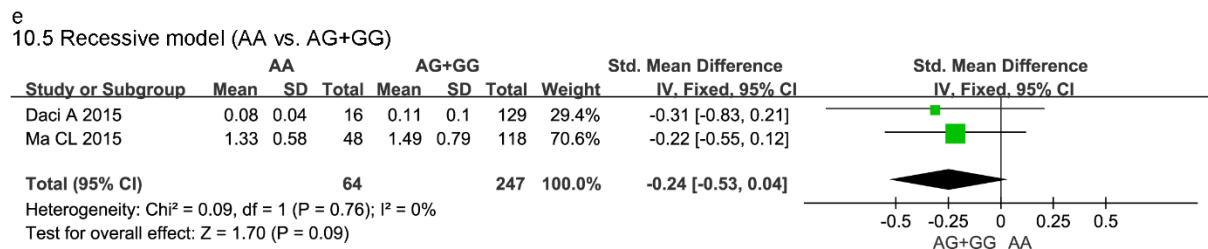
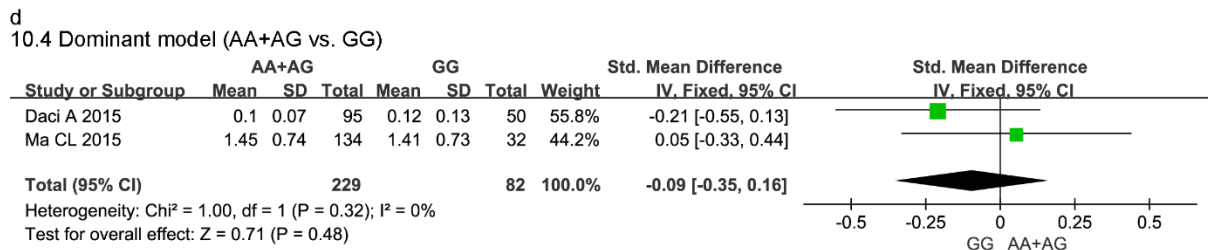
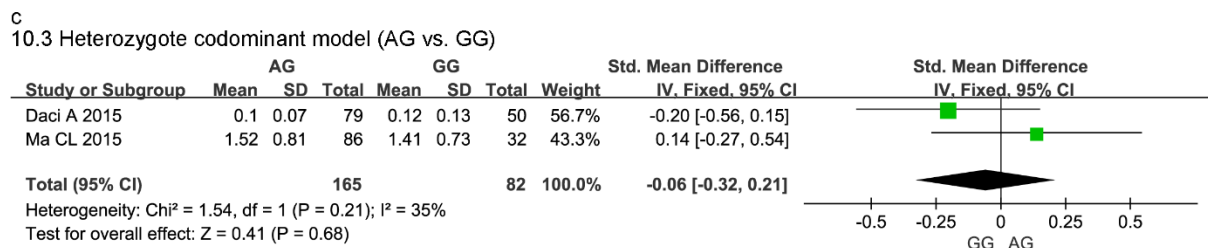
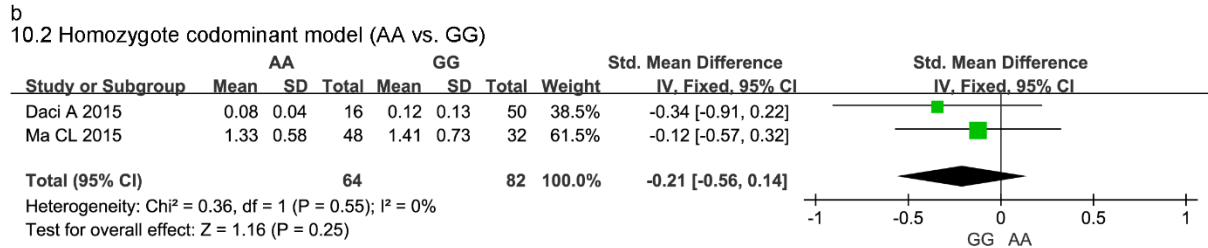
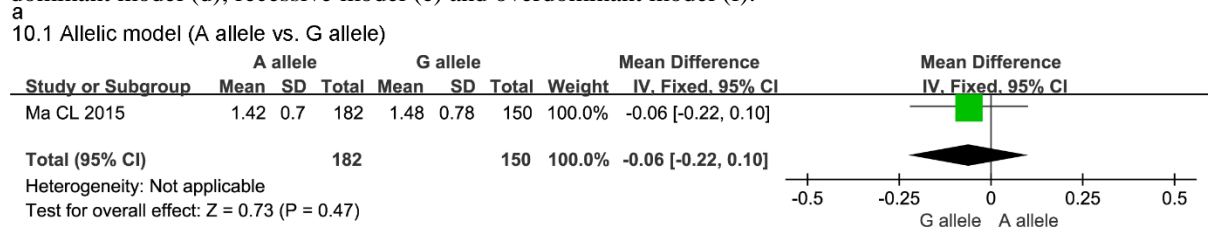


e

13.5 Overdominant model (AG vs. AA+GG)



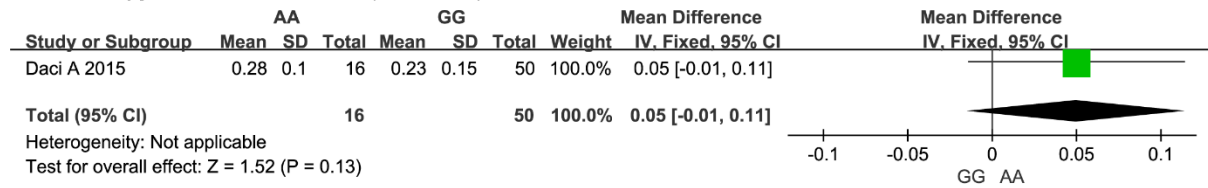
Supplemental Fig. S.10 Forest plot for association between SCN1A rs3812718 polymorphism and plasma CBZE concentration in allelic model (a), homozygote codominant model (b), heterozygote codominant model (c), dominant model (d), recessive model (e) and overdominant model (f).



Supplemental Fig. S.11 Forest plot for association between SCN1A rs3812718 polymorphism and plasma CBZD concentration in homozygote codominant model (a), heterozygote codominant model (b), dominant model (c), recessive model (d) and overdominant model (e).

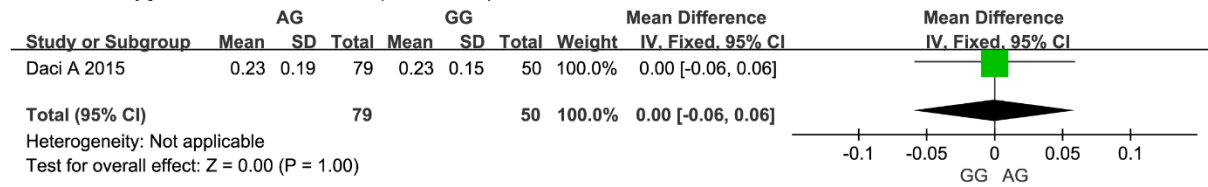
a

11.1 Homozygote codominant model (AA vs. GG)



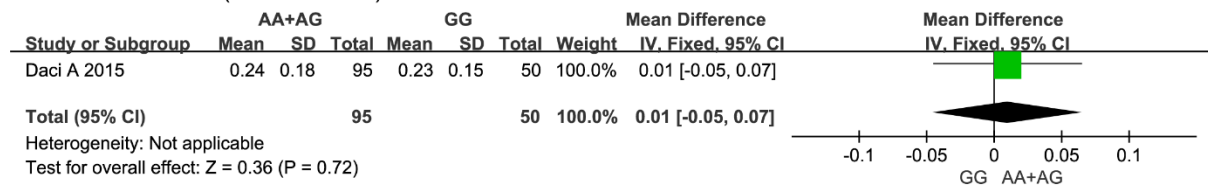
b

11.2 Heterozygote codominant model (AG vs. GG)



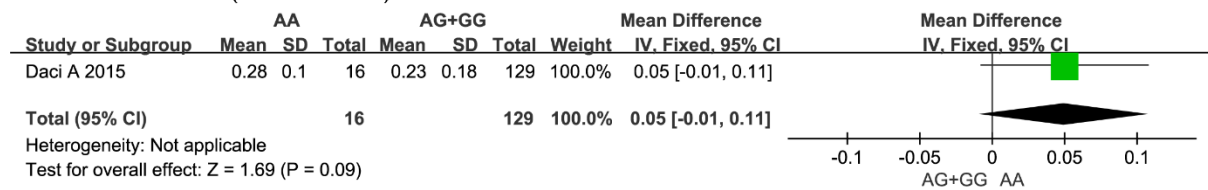
c

11.3 Dominant model (AA+AG vs. GG)



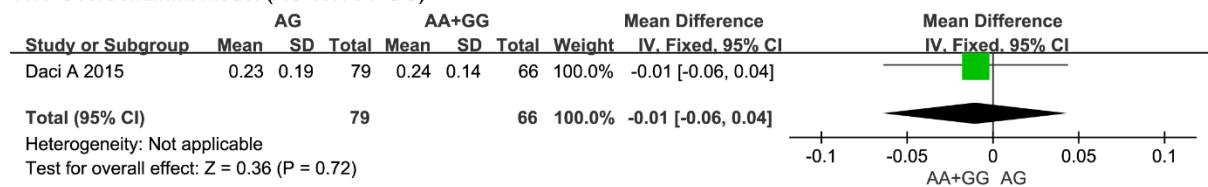
d

11.4 Recessive model (AA vs. AG+GG)



e

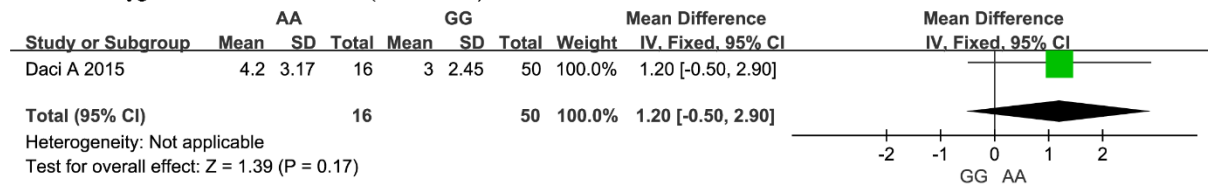
11.5 Overdominant model (AG vs. AA+GG)



Supplemental Fig. S.12 Forest plot for association between SCN1A rs3812718 polymorphism and plasma concentration of CBZD to CBZE ratio in homozygote codominant model (a), heterozygote codominant model (b), dominant model (c), recessive model (d) and overdominant model (e).

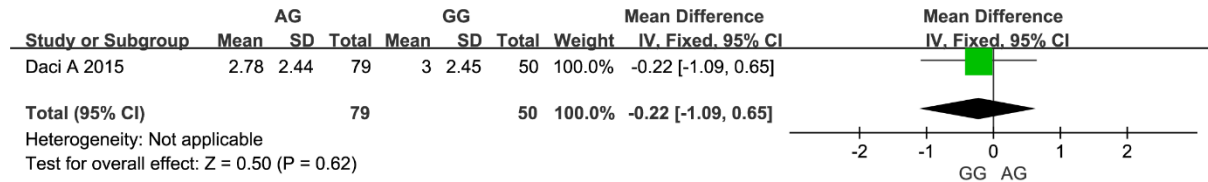
a

14.1 Homozygote codominant model (AA vs. GG)



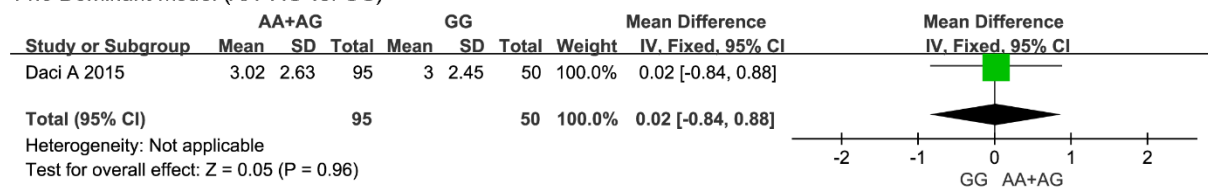
b

14.2 Heterozygote codominant model (AG vs. GG)



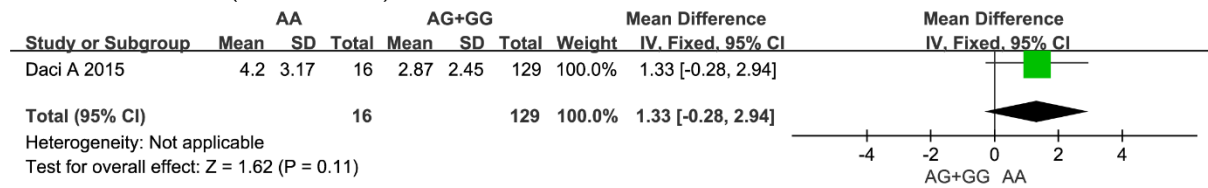
c

14.3 Dominant model (AA+AG vs. GG)



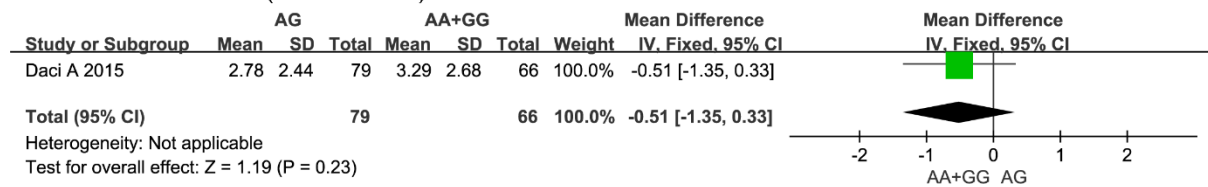
d

14.4 Recessive model (AA vs. AG+GG)

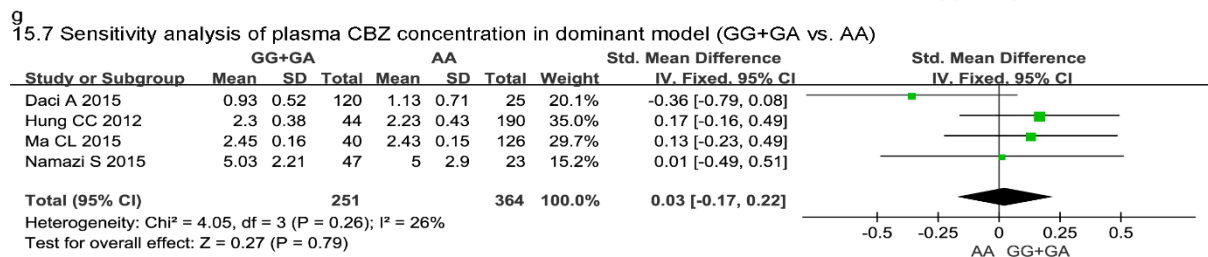
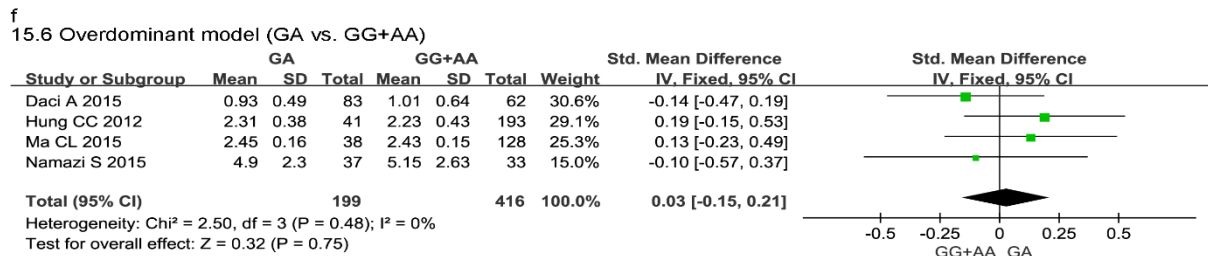
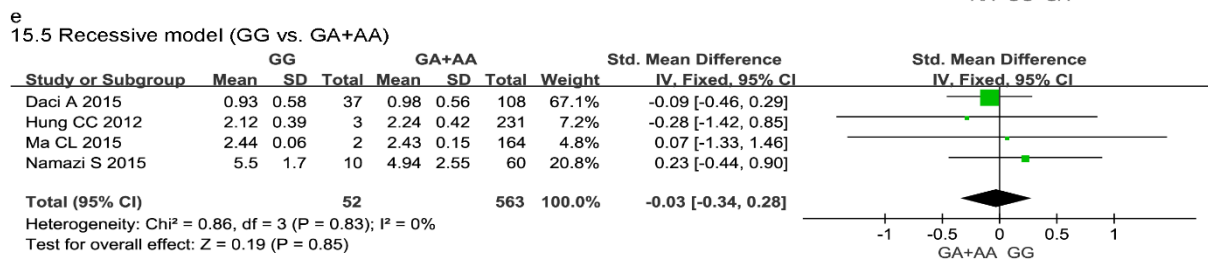
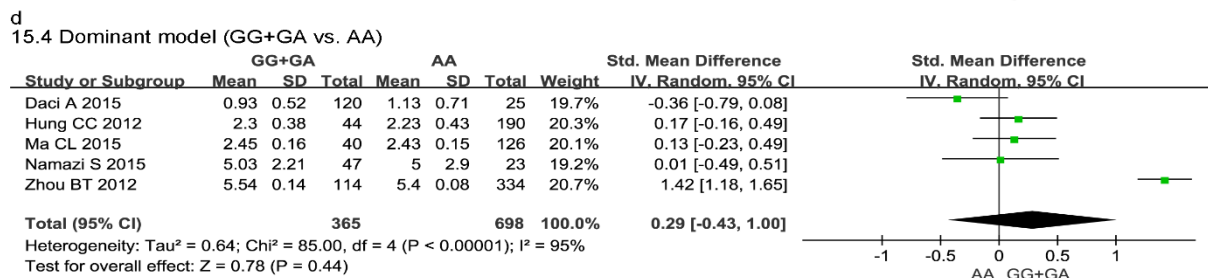
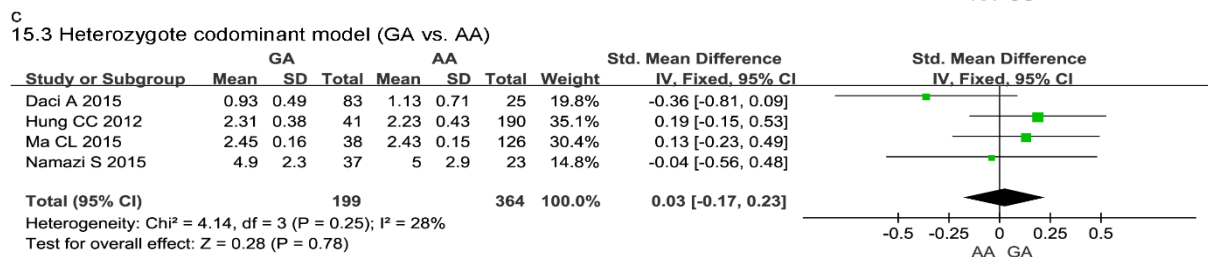
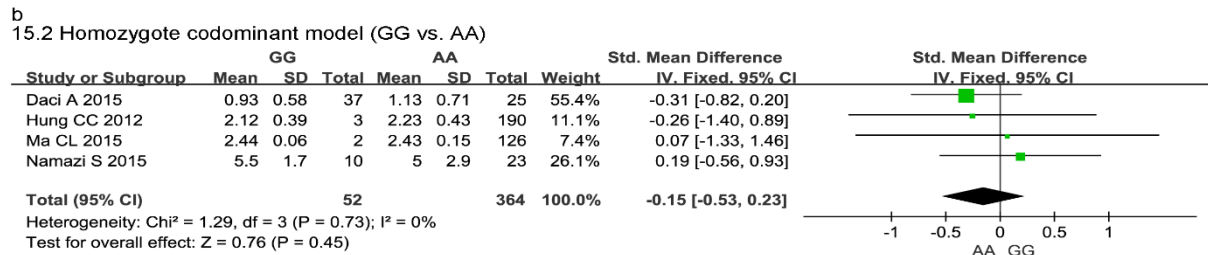
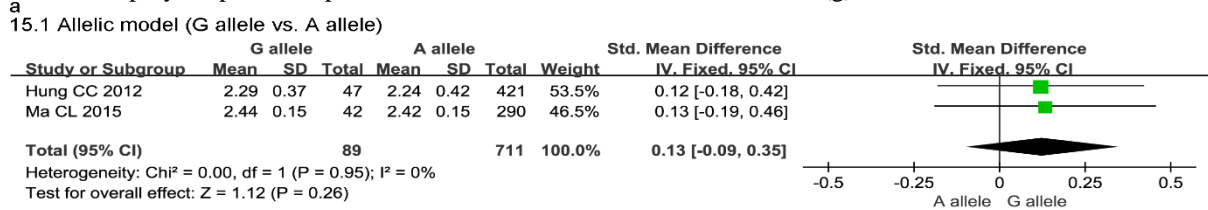


e

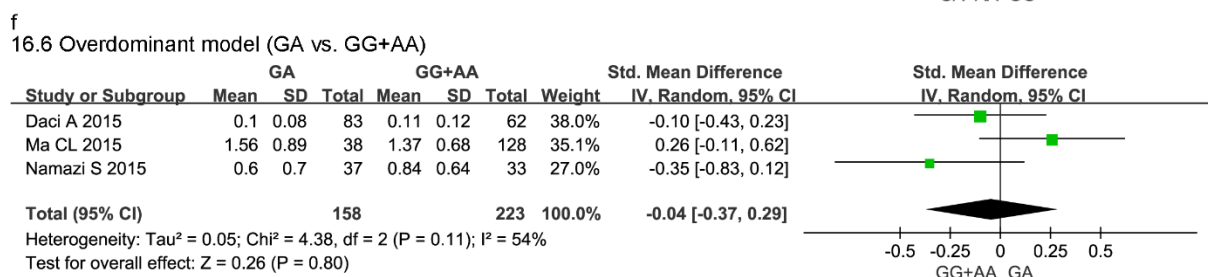
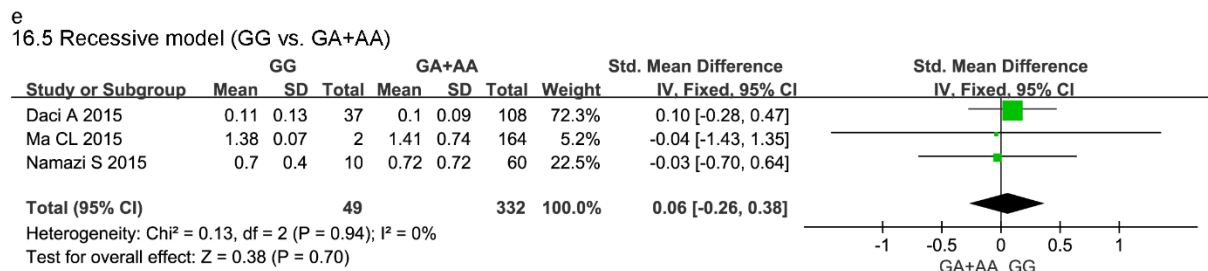
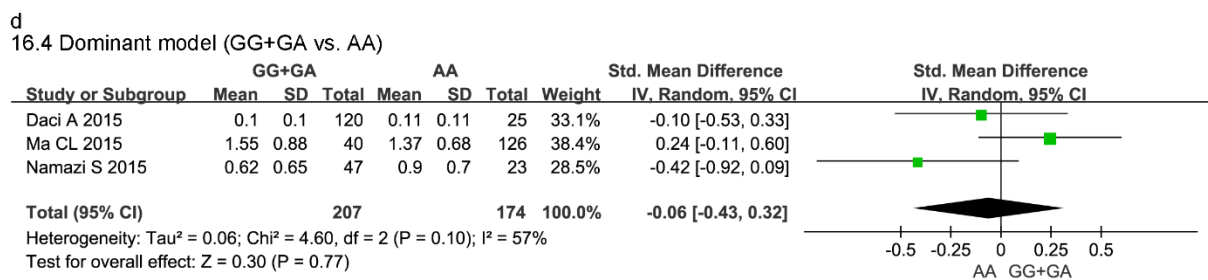
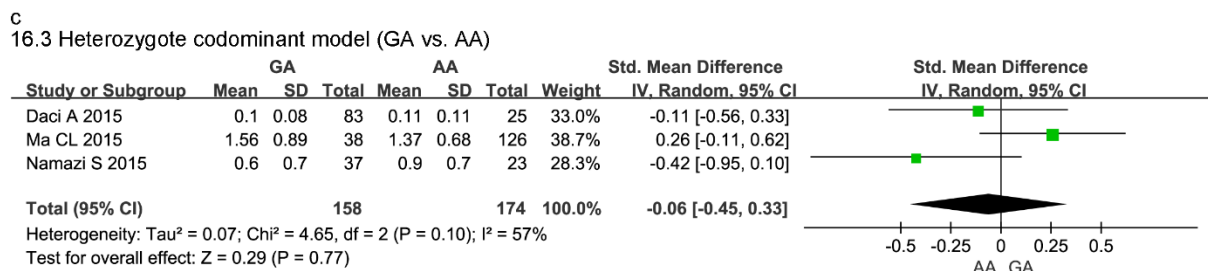
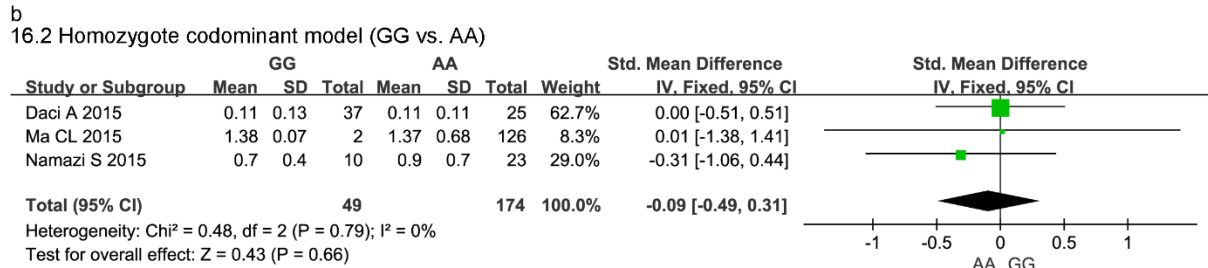
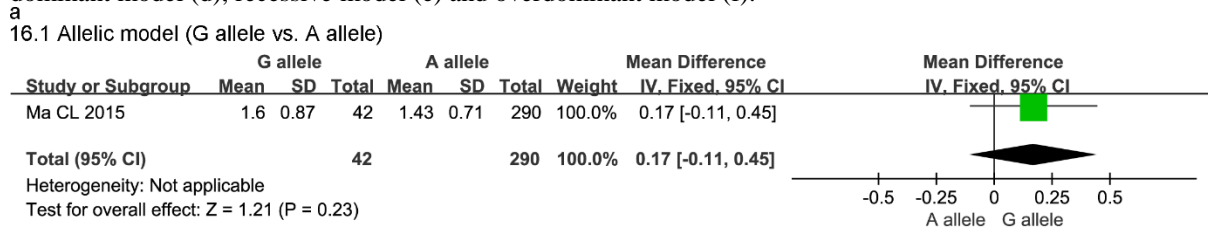
14.5 Overdominant model (AG vs. AA+GG)



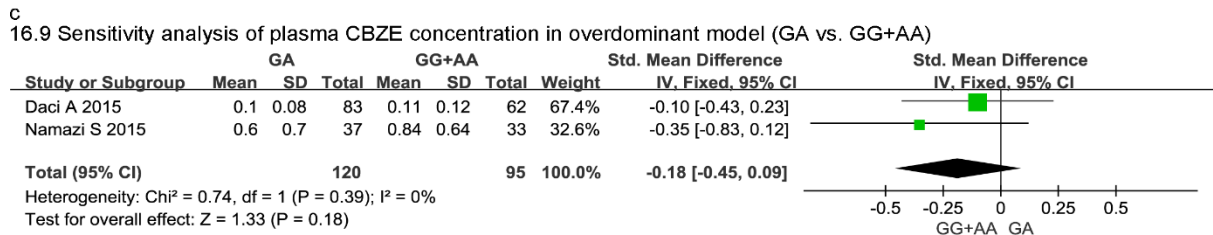
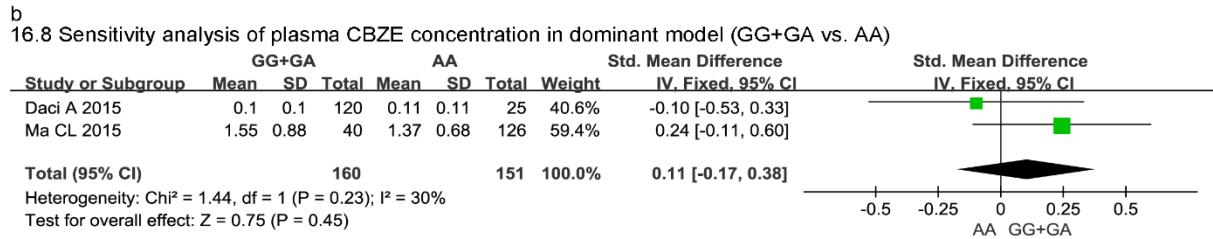
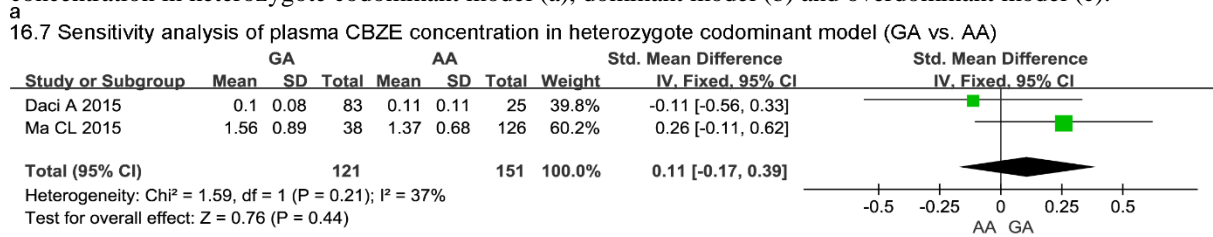
Supplemental Fig. S.13 Forest plot for association between SCN1A rs2298771 polymorphism and plasma CBZ concentration in allelic model (a), homozygote codominant model (b), heterozygote codominant model (c), dominant model (d), recessive model (e) and overdominant model (f). Sensitivity analysis for effect of SCN1A rs2298771 polymorphism on plasma CBZ concentration in recessive model (g).



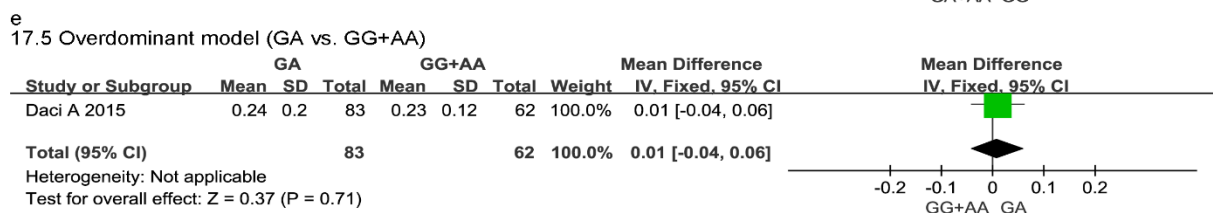
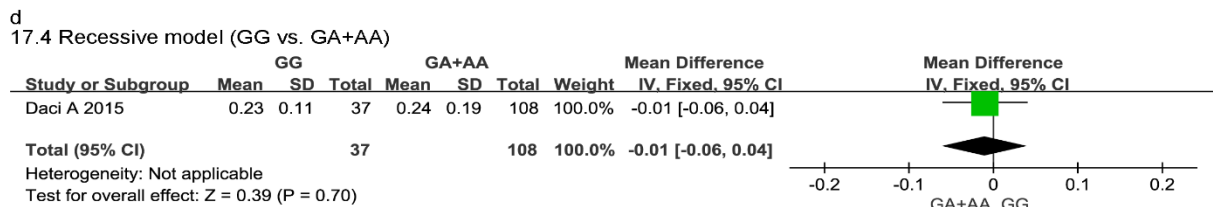
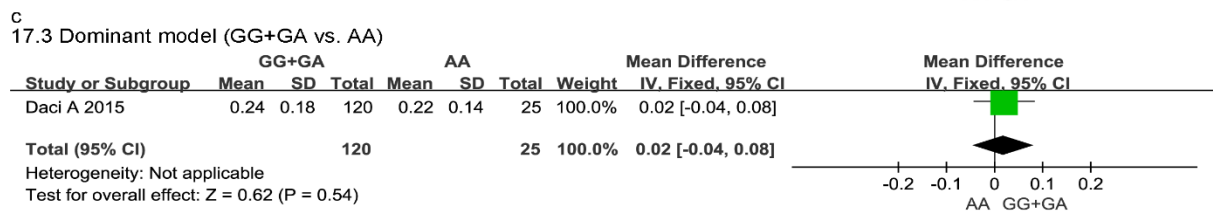
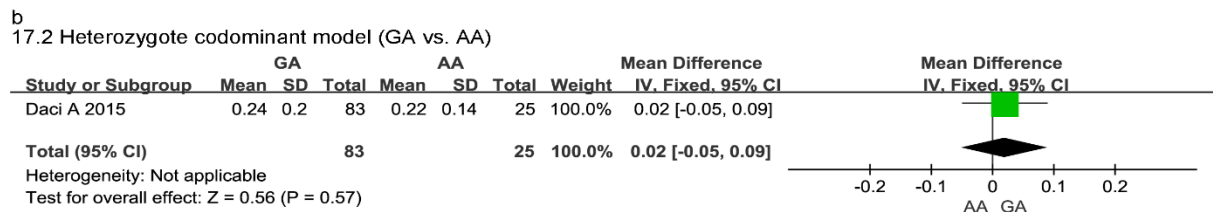
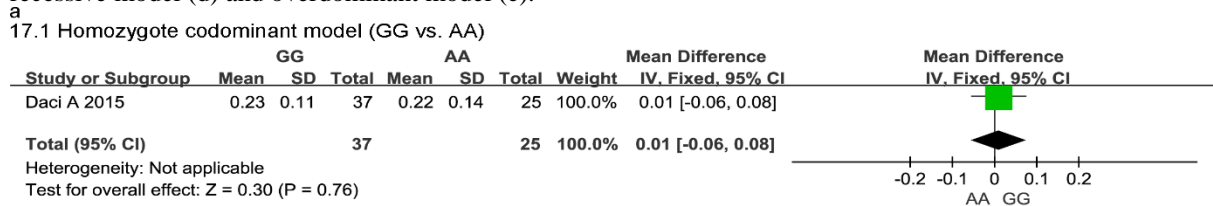
Supplemental Fig. S.14 Forest plot for association between SCN1A rs2298771 polymorphism and plasma CBZE concentration in allelic model (a), homozygote codominant model (b), heterozygote codominant model (c), dominant model (d), recessive model (e) and overdominant model (f).



Supplemental Fig. S.15 Sensitivity analysis for effect of SCN1A rs2298771 polymorphism on plasma CBZE concentration in heterozygote codominant model (a), dominant model (b) and overdominant model (c).



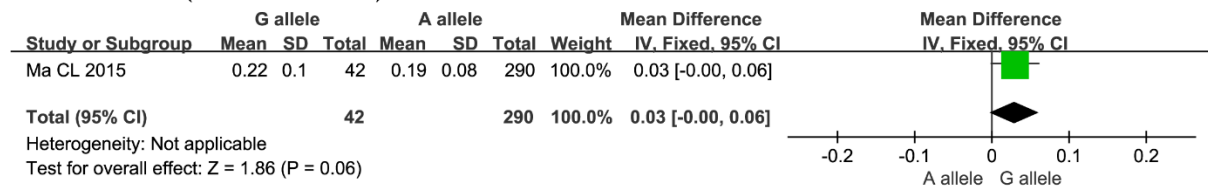
Supplemental Fig. S.16 Forest plot for association between SCN1A rs2298771 polymorphism and plasma CBZD concentration in homozygote codominant model (A), heterozygote codominant model (b), dominant model (c), recessive model (d) and overdominant model (e).



Supplemental Fig. S.17 Forest plot for association between SCN1A rs2298771 polymorphism and plasma concentration of CBZE to CBZ ratio in allelic model (a), homozygote codominant model (b), heterozygote codominant model (c), dominant model (d), recessive model (e) and overdominant model (f).

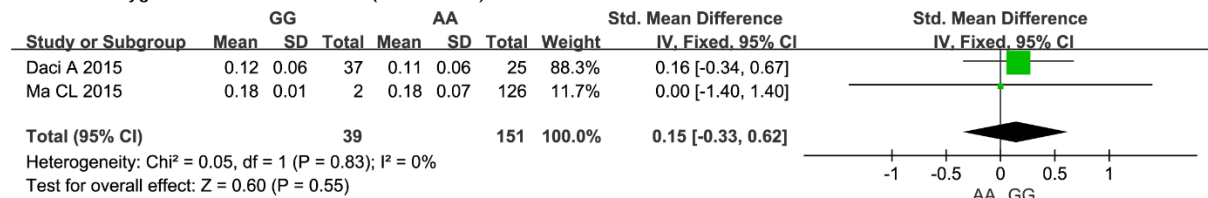
a

18.1 Allelic model (G allele vs. A allele)



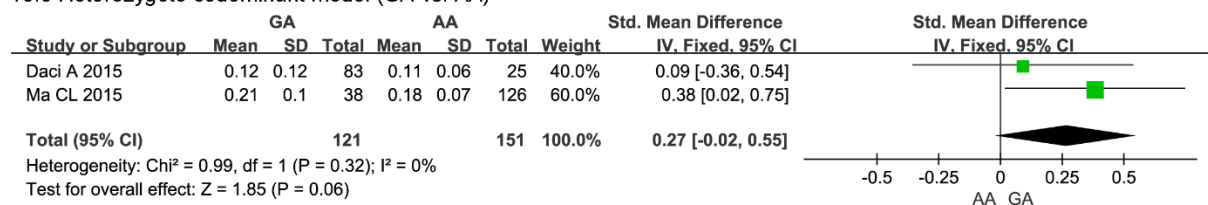
b

18.2 Homozygote codominant model (GG vs. AA)



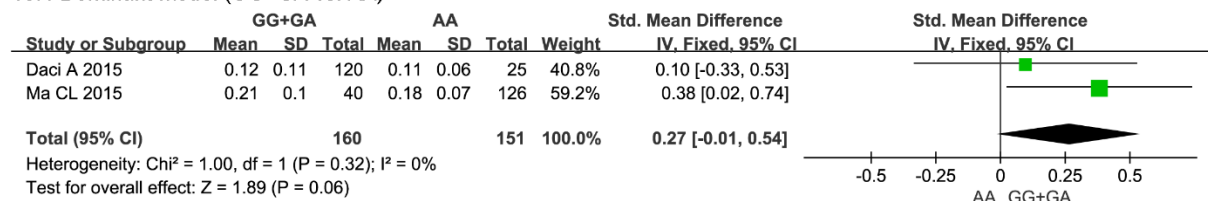
c

18.3 Heterozygote codominant model (GA vs. AA)



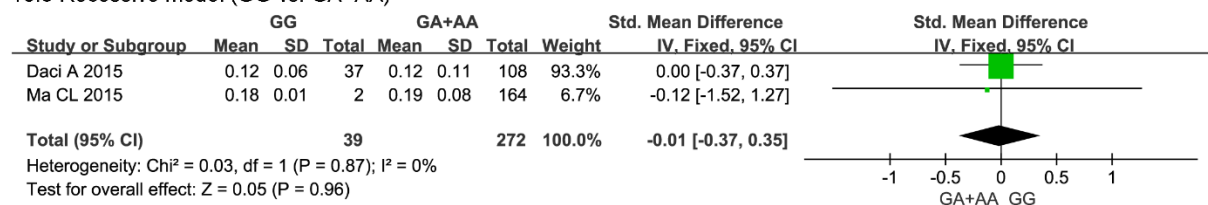
d

18.4 Dominant model (GG+GA vs. AA)



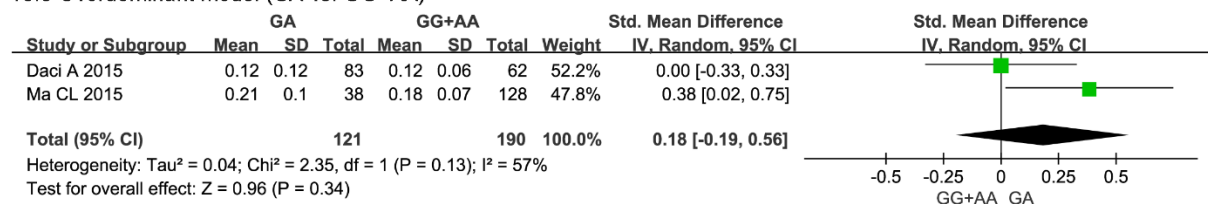
e

18.5 Recessive model (GG vs. GA+AA)

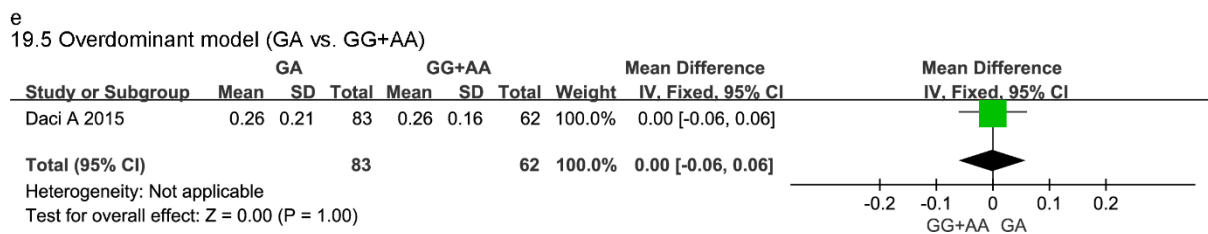
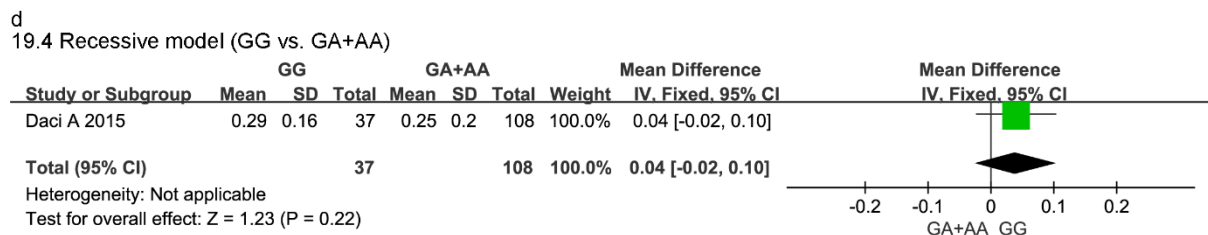
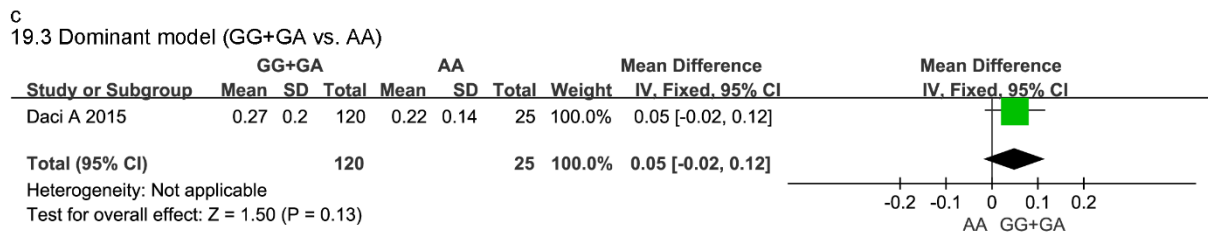
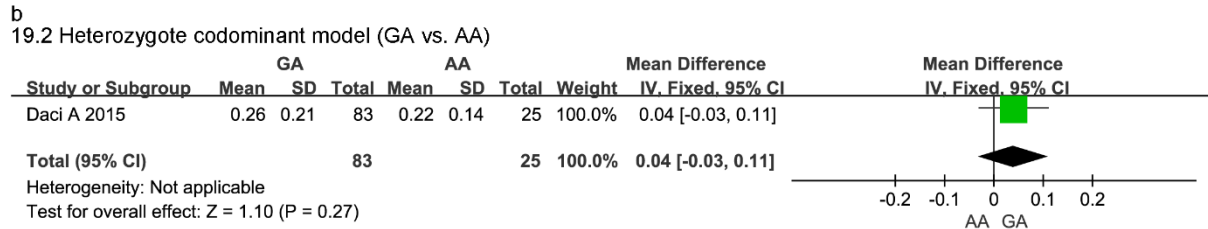
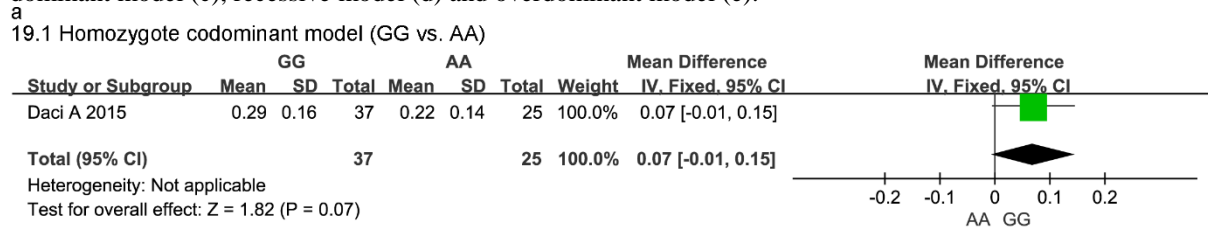


f

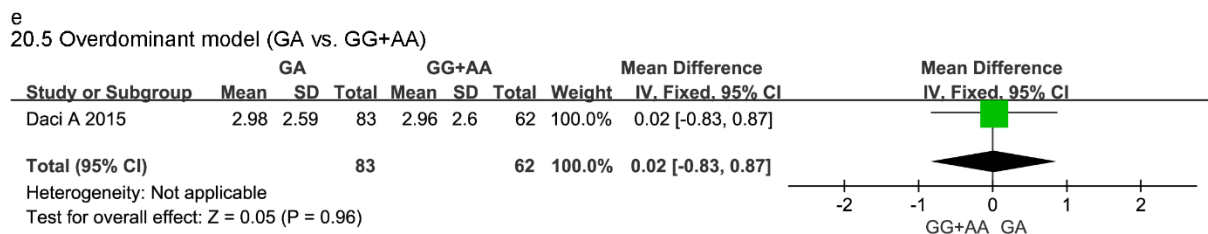
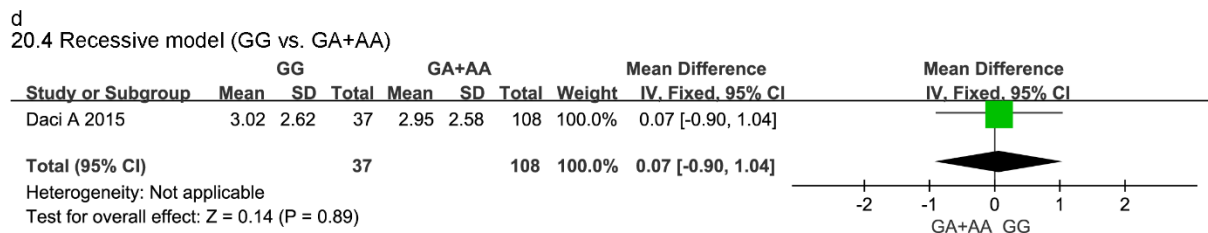
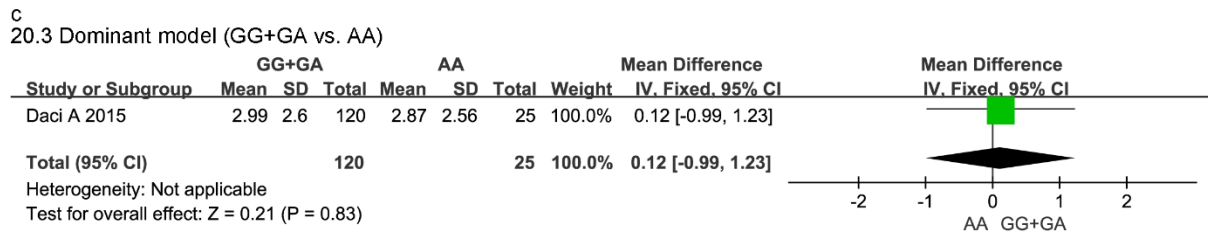
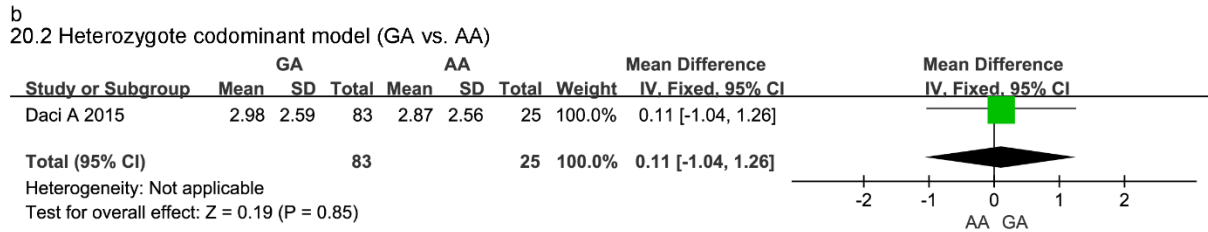
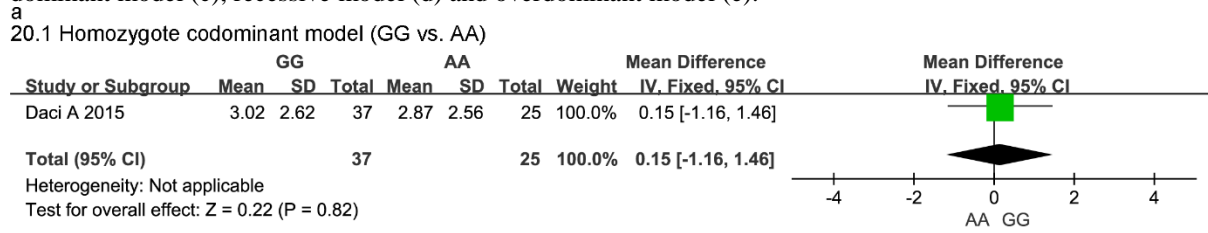
18.6 Overdominant model (GA vs. GG+AA)



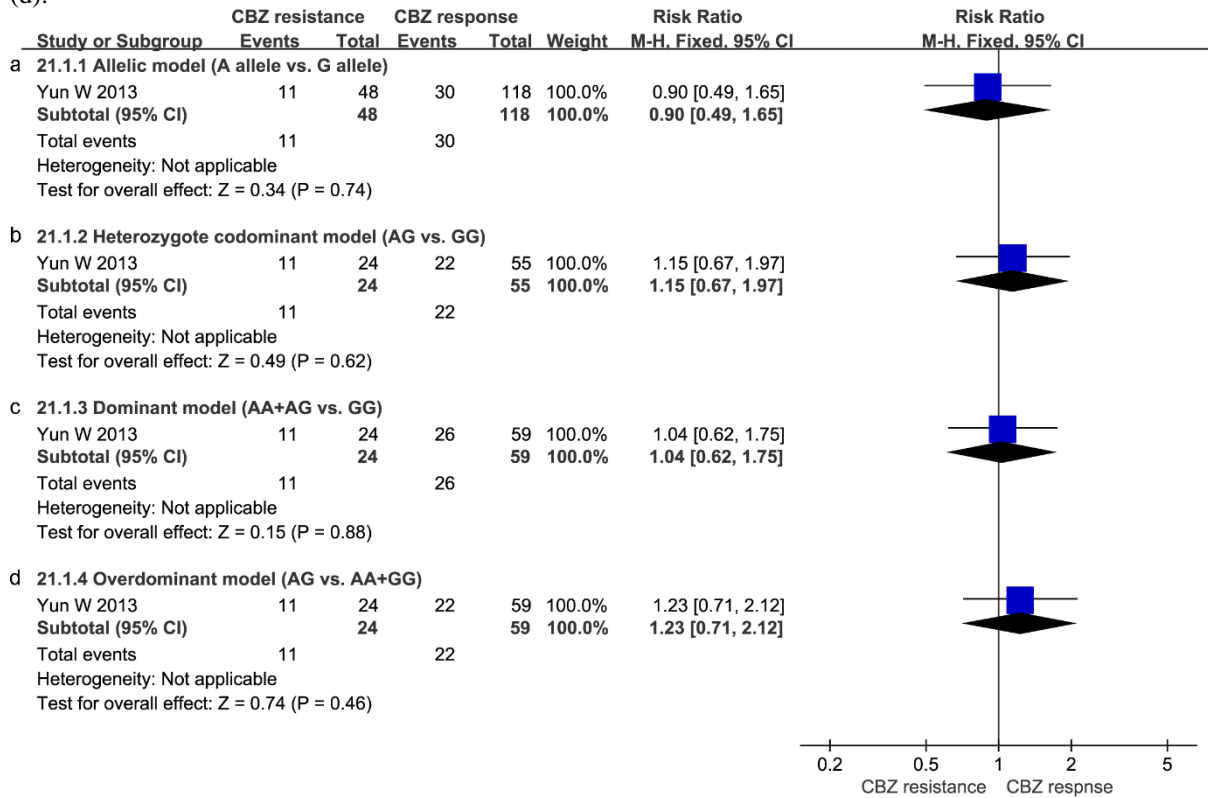
Supplemental Fig. S.18 Forest plot for association between SCN1A rs2298771 polymorphism and plasma concentration of CBZD to CBZ ratio in homozygote codominant model (a), heterozygote codominant model (b), dominant model (c), recessive model (d) and overdominant model (e).



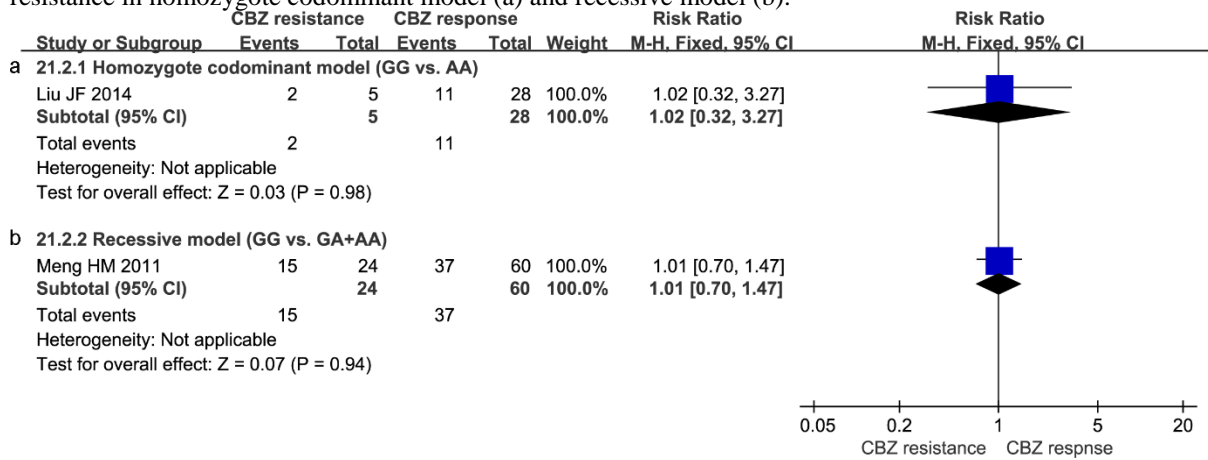
Supplemental Fig. S.19 Forest plot for association between SCN1A rs2298771 polymorphism and plasma concentration of CBZD to CBZE ratio in homozygote codominant model (a), heterozygote codominant model (b), dominant model (c), recessive model (d) and overdominant model (e).



Supplemental Fig. S.20 Forest plot for association between CYP3A4 rs2242480 polymorphism and CBZ resistance in allelic model (a), heterozygote codominant model (b), dominant model (c) and overdominant model (d).



Supplemental Fig. S.21 Forest plot for association between CYP3A5 rs776746 polymorphism and CBZ resistance in homozygote codominant model (a) and recessive model (b).



Supplemental Fig. S.22 Forest plot for association between SCN1A rs2298771 polymorphism and CBZ resistance in allelic model (a), homozygote codominant model (b), heterozygote codominant model (c), dominant model (d), recessive model (e) and overdominant model (f). Sensitivity analysis for effect of SCN1A rs2298771 polymorphism on CBZ resistance in dominant model (g).

